n-type to *p*-type crossover in quaternary $Bi_xSb_yPb_zSe_3$ single crystals

J. Kašparová, Č. Drašar,[a] and A. Krejčová
Faculty of Chemical Technology, University of Pardubice, Čs. Legií Square 565, 532 10 Pardubice, Czech Republic

L. Beneš
Joint Laboratory of Solid State Chemistry of the Institute of Macromolecular Chemistry of the Academy of Sciences of the Czech Republic and the University of Pardubice, Studentská 84, 532 10 Pardubice, Czech Republic

P. Lošťák
Faculty of Chemical Technology, University of Pardubice, Čs. Legií Square 565, 532 10 Pardubice, Czech Republic

Wei Chen, Zhenhua Zhou, and C. Uher
Department of Physics, University of Michigan, Ann Arbor, Michigan 48109-1120

(Received 11 November 2004; accepted 15 March 2005; published online 11 May 2005)

We report on the preparation and some physical properties of a quaternary system based on Bi_2Se_3 codoped with Sb and Pb. Single-crystal samples were prepared using the Bridgman technique and were characterized by measurements of the lattice parameters, electrical resistivity, Hall coefficient, Seebeck coefficient, and thermal conductivity. Atomic emission spectroscopy was used to find the concentration profiles of Sb and Pb along the single-crystalline ingots. Progressive codoping of the Bi_2Se_3 crystal lattice with Sb and Pb leads to a crossover of the initially *n*-type conduction to that of the *p* type. It is assumed that both Sb and Pb enter the Bi sublattice. Physical properties as well as the change in the dominant carrier type are discussed. © *2005 American Institute of Physics*. [DOI: 10.1063/1.1904158]

I. INTRODUCTION

Bismuth selenide (Bi_2Se_3) belongs to the family of narrow-band semiconductors $A_2^VB_3^{VI}$ (A=Bi,Sb and B=Se, Te) with the tetradymite structure (space group D_{3d}^5) that form the base materials for room-temperature thermoelectric devices.[1] Therefore, both the parent binary materials as well as their solid solutions are of theoretical and practical interest.

It is known that as-grown Bi_2Se_3 is a degenerate *n*-type semiconductor with electron concentration $n \approx 10^{19}$ cm^{-3}. Such a high electron concentration results from the predominance of one type of native defect—selenium vacancies ($V_{Se}^{\bullet\bullet}$) that produce electrons—over another type—bismuth antisite defects ($Bi_{Se}^{/}$). Predominance of selenium vacancies makes it very difficult to prepare *p*-type Bi_2Se_3 and in spite of the considerable attention devoted to this compound and its solid solutions,[2,3] there is little information about *p*-type materials based on Bi_2Se_3.[4,5] According to Ref. 6, there is a noticeable decrease in electron concentration upon alloying Bi_2Se_3 with Sb_2Se_3, thanks to the suppression of native defects. Moreover, doping with Pb leads to a decrease in electron concentration via the creation of point defect $Pb_{Bi}^{/}$.[7] With the aim of preparing *p*-type single crystals based on Bi_2Se_3, we investigated the influence of double doping with Sb and Pb on the physical properties of the parent Bi_2Se_3. Changes in the free-carrier concentration and a crossover to the *p*-type conduction are discussed within the framework of point defects.

[a]Electronic mail: cestmir.drasar@upce.cz

II. EXPERIMENTAL PROCEDURE

A. *Preparation of single crystals*

Single crystals of the quaternary system were pulled using a modified Bridgman technique described elsewhere.[8] The crystals obtained (ingot length of 50 mm and diameter of 10 mm) cleaved easily along the (0001) planes. $(Bi_{0.75}Sb_{0.25})_{2-z}Pb_zSe_3$, with z varying from 0 to 0.04, was the nominal composition of all the crystals investigated.

B. *Characterization of the crystals*

The crystals were characterized by the x-ray diffraction (XRD) structural analysis and by the measurements of electrical resistivity $\rho_{\perp c}$, Hall coefficient $R_H(B \| c)$, Seebeck coefficient $\alpha(\Delta T \perp c)$, and thermal conductivity $\kappa(\Delta T \perp c)$ in the temperature range 2-300 K. These experimental techniques are described elsewhere.[9] The actual sample composition was determined using the atomic emission spectroscopy (AES) and is designated by the formula $Bi_xSb_yPb_zSe_3$, where $x+y+z=2$. The same technique was used for the measurement of concentration profiles of the doping elements along the pulling axis.

III. RESULTS AND DISCUSSION

A. *Lattice parameters*

X-ray diffractograms for the parent Bi_2Se_3, the ternary sample $(Bi_{0.75}Sb_{0.25})_2Se_3$, and the quaternary sample $(Bi_{0.75}Sb_{0.25})_{2.96}Pb_{0.04}Se_3$ with the highest content of lead are depicted in Fig. 1. They indicate that no secondary phases

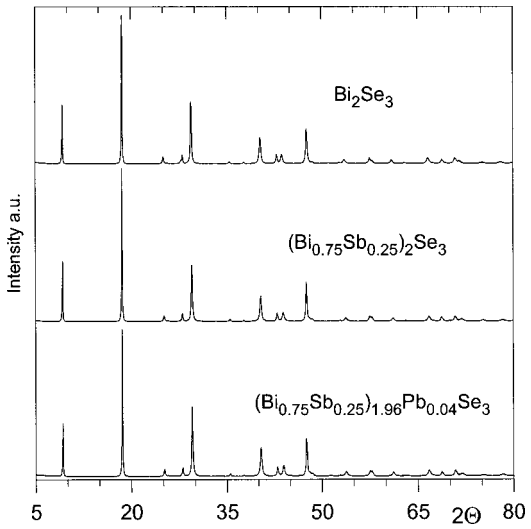

FIG. 1. X-ray diffractograms of Bi_2Se_3 ternary sample $(Bi_{0.75}Sb_{0.25})_2Se_3$ and quaternary sample $(Bi_{0.75}Sb_{0.25})_{2-z}Pb_zSe_3$ with highest content of Pb.

are present in the as-grown crystals. The lattice parameters are summarized in Table I. In agreement with Ref. 6, the unit-cell volume of the ternary system $(Bi_{0.75}Sb_{0.25})_2Se_3$ is smaller than that of Bi_2Se_3. Upon doping with Pb, we observe no change in the unit-cell volume because the concentration of Pb is too small and the radii of Pb and Bi are comparable.

B. *Homogeneity of the crystals*

Since the Bridgman crystal growth is essentially a directional solidification, great attention was paid to mapping the concentration gradient of the component elements along the pulling direction. As described in Ref. 6, there is a gradient of Sb and Bi in $(Bi_{1-y}Sb_y)_2Se_3$ single crystals along the pulling direction. The concentration profiles of Sb and Pb along the pulling direction for a quaternary $(Bi_{0.75}Sb_{0.25})_{2.96}Pb_{0.04}Se_3$ crystal are depicted in Fig. 2. One observes a practically constant concentration of the elements for the first 40 mm measured from the tip of the single crystal. It is only in the last 10–15 mm (the head of the single crystal) where concentrations of the dopants change markedly. This fact facilitates reproducible preparation of single crystals with the desired composition. The concentration profiles with a plateau are characteristic of these Bridgman technique-grown crystals. Interestingly, both Sb and Pb show the same tendency of increasing concentration from the tip to the head of single crystals. The head segment of single crystals crystallizes as a multiphased solid (x-ray diffraction data

TABLE I. Lattice parameters (average value) of the $(Bi_{0.75}Sb_{0.25})_{2-z}Pb_zSe_3$ single crystals.

Nominal composition	a (nm)	c (nm)	c/a	V (nm^3)
Bi_2Se_3	0.413 86(4)	2.862 0(2)	6.915(2)	0.424 50(5)
$(Bi_{0.75}Sb_{0.25})_2Se_3$	0.412 15(2)	2.866 1(1)	6.954(2)	0.421 62(5)
$(Bi_{0.75}Sb_{0.25})_{1.98}Pb_{0.02}Se_3$	0.412 20(3)	2.865 9(2)	6.953(2)	0.421 71(7)
$(Bi_{0.75}Sb_{0.25})_{1.96}Pb_{0.04}Se_3$	0.412 10(3)	2.866 6(2)	6.954(2)	0.421 59(7)

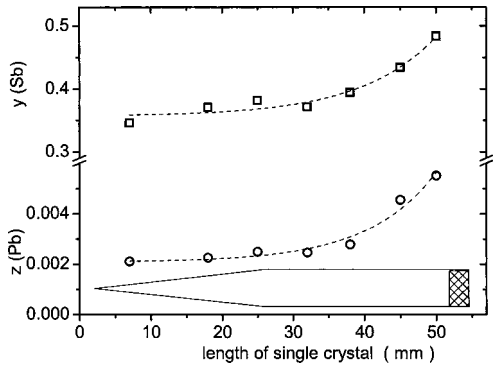

FIG. 2. The concentration profiles for Sb and Pb along a single crystal of $(Bi_{0.75}Sb_{0.25})_{1.96}Pb_{0.04}Se_3$. The drawing below represents the single crystal with segregated many-phase solid at the head of the crystal (shaded).

indicate the presence of Bi_2Se_3, Sb_2Se_3, and $Pb_2Bi_2Se_5$) with an enhanced concentration of lead and antimony (see Fig. 3). The profiles allow us to estimate the maximum solubility of the elements in the Bi_2Se_3 matrix—the estimates yield $z_{max} \approx 0.006$ for Pb and $y_{max} \approx 0.5$ for Sb. The latter value is higher than the solubility reported in Ref. 10, where $y_{max} \approx 0.33$ was given for polycrystalline $Bi_{2-y}Sb_ySe_3$ samples. According to the phase diagram[10] the solubility of Sb increases with temperature. Thus, a possible explanation is that the single crystals are frozen at elevated temperatures. Upon inspecting Fig. 2, it is clear that the concentrations of Pb and Sb along the length of the ingot do not reach the nominal sample concentrations. The actual compositions of all measured samples are summarized in Table II.

C. *Transport coefficients*

The results of the measurements of temperature dependence of electrical resistivity $\rho_{\perp c}$, Hall coefficient $R_H(B \| c)$, Seebeck coefficient $\alpha(\Delta T \perp c)$, and thermal conductivity $\kappa(\Delta T \perp c)$ are depicted in Figs. 4–7. The curves are numbered according to Table II. From the changes of the Hall and Seebeck coefficients, it is evident that with the increasing content of Pb the concentration of electrons in the initially *n*-type material decreases and the system converts to *p*-type conduction at the highest content of Pb. The results of electrical resistivity also indicate this trend. The decrease in the peak value of the thermal conductivity and a shift of the peak towards higher temperatures indicate the increased influence of point defect scattering with the increasing concentration of Pb in the sample. The decrease in the concentration of electrons upon Pb doping could be explained in terms of point defects (see Sec. III D below). The sample of special interest is the intermediate sample 4, which shows *p*-type

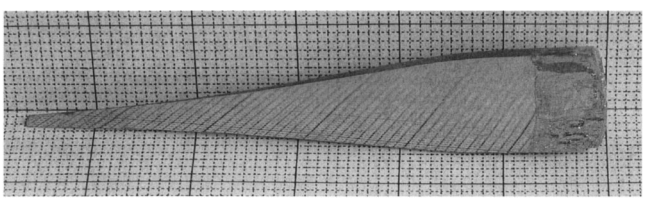

FIG. 3. Photograph of cleaved single crystal of $(Bi_{0.75}Sb_{0.25})_{1.96}Pb_{0.04}Se_3$. Note the multiphase solid at the head of the crystal.

TABLE II. Actual composition of $Bi_xSb_yPb_zSe_3$ single crystals (estimated errors ±15%).

Sample No.	x	y/wt. %	z/wt. %
1	1.6	0.40/7.9	0/0
2	1.63	0.37/7.2	0.001 2/0.039
3	1.63	0.37/7.2	0.001 6/0.052
4	1.63	0.37/7.2	0.001 8/0.059
5	1.59	0.41/8.1	0.003 2/0.106

conduction at low temperatures that changes into an electron-dominated conduction at elevated temperatures.

D. *Point defects*

From Figs. 4–6 it is evident that upon doping with Pb the concentration of electrons decreases and the initially *n*-type material crosses over to *p*-type conduction. In this section we shall attempt to explain qualitatively this process.

We start by assuming that the concentration of free-charge carriers in the crystals of $(Bi_{1-x}Sb_x)_2Se_3$ is given by the concentration and character of native point defects just as was the case of Bi_2Se_3. It is well known that Bi_2Se_3 grown from stoichiometric melts reveals overstoichiometric content of Bi.[11] In agreement with Ref. 12 this leads to the creation of native point defects, namely, negatively charged antisite defects Bi'_{Se} and positively charged selenium vacancies V^{**}_{Se}. The concentration of V^{**}_{Se} exceeds the concentration of Bi'_{Se} so that the concentration of free electrons is given by the following equation

$$[e'] = 2[V^{**}_{Se}] - [Bi'_{Se}]. \quad (1)$$

The influence of Sb on the transport properties of Bi_2Se_3 is indirect because Sb is isoelectronic with Bi and such substitution in itself produces no free carriers. Nevertheless, it is observed that low concentrations of Sb lead to an increase in electron concentration, whereas higher concentrations result in a decrease of electron concentration. According to Refs. 6 and 13, this effect was explained by means of the interaction of Sb with native defects Bi'_{Se} and V^{**}_{Se}. It was assumed that the increasing concentration of uncharged substitutional defects Sb^x_{Bi} tends to suppress the negatively charged antisite defects as well as selenium vacancies.

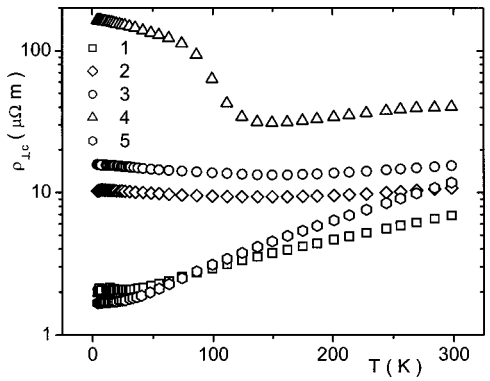

FIG. 4. Electrical resistivity $\rho_{\perp c}$ as a function of temperature for crystals of $Bi_xSb_yPb_zSe_3$. The curves are numbered according to Table II.

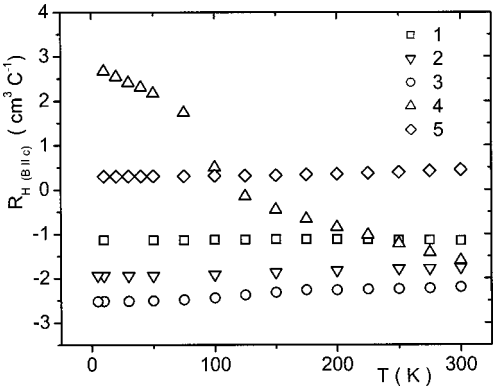

FIG. 5. Hall coefficient $R_H(B\|c)$ as a function of temperature for crystals of $Bi_xSb_yPb_zSe_3$. The curves are numbered according to Table II.

Next we suppose that Pb, just as Sb, is located exclusively on the sublattice of Bi. Comparison of the crystal radii $r(Bi^{+3}) = 0.103$ nm, $r(Pb^{+2}) = 0.117$ nm, and $r(Se^{-2}) = 0.184$ nm supports the idea. The first process that accounts for the decrease in electron concentration is due to Pb entering the Bi sublattice. In the process it creates negatively charged substitutional point defects Pb'_{Bi} that yield holes h^* according to the following equation

$$2Pb + 3Se \rightarrow 2Pb'_{Bi} + Bi_2Se_3 + 2h^*. \quad (2)$$

The holes recombine with electrons and decrease their concentration. We cannot exclude the interaction of Pb'_{Bi} defects with vacancies V^{**}_{Se}, which is another process that might possibly explain the decrease in the concentration of electrons. The change in electron concentration Δn as a function of Pb concentration c_{Pb} at room temperature is plotted in Fig. 8. We define $\Delta n = n_0 - n$, where n_0 and n are the concentrations of the electrons in the sample $(Bi_{0.75}Sb_{0.25})_2Se_3$ and Pb-doped samples, respectively. We note that one atom of Pb produces approximately 0.25 holes, which contradicts Eq. (2). This apparent reduction in the activity of Pb can be explained in terms of the results presented in Ref. 14. Accordingly, elements of group IV (Ge, Sn, and Pb) produce the so-called seven-layer-lamellae structure *B-A-B-M-B-A-B* (where *B* = Te,Se; *A* = Sb,Bi, and *M* = Ge,Sn,Pb) in the tetradymite crystals. Thus, we assume that a large fraction of Pb atoms is incorporated in the crystal lattice as electrically inactive seven-layer-lamellae Se-Bi(Sb)-Se-Pb-Se-Bi(Sb)-Se. We

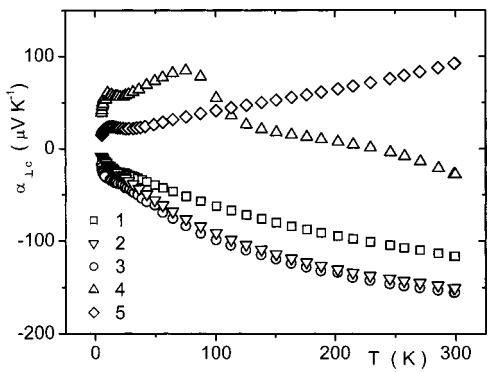

FIG. 6. Seebeck $\alpha(\Delta T \perp c)$ coefficient as a function of temperature for crystals of $Bi_xSb_yPb_zSe_3$. The curves are numbered according to Table II.

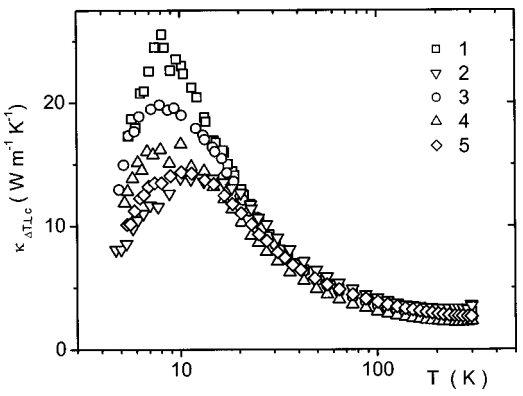

FIG. 7. Thermal conductivity $\kappa(\Delta T \perp c)$ as a function of temperature for crystals of $Bi_xSb_yPb_zSe_3$. The curves are numbered according to Table II.

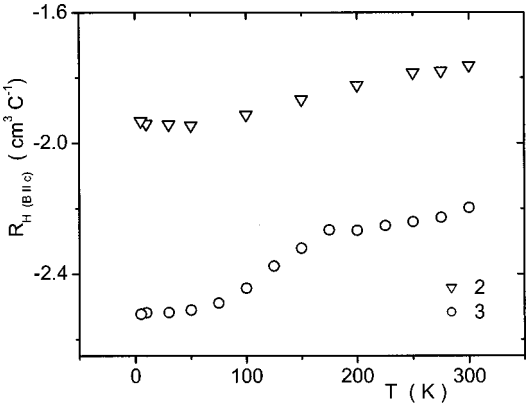

FIG. 9. Hall coefficient as a function of temperature—an expanded scale for samples 2 and 3.

note that a similar effect was observed in Ge-doped Bi_2Te_3.[15]

The above arguments can qualitatively account for the behavior of all samples, except sample 4. Measurements of $\rho_{\perp c}=f(T)$, $R_H(B\|c)=f(T)$, and $\alpha(\Delta T \perp c)=f(T)$ on this sample show an anomalous temperature dependence (Figs. 4–6), which can indicate a donor level activated at $T \approx 70$ K. A drop in the Hall coefficient is also noticeable in samples 2 and 3, as detailed in Fig. 9. We cannot exclude a possibility that the anomalous behavior of the transport properties is connected with the formation of a defect in the crystal structure. One possible candidate is a complex defect consisting of a substitutional defect and a selenium vacancy ($Pb_{Bi}V_{Se}$).

However, the temperature dependence of the transport properties can also result from the band structure complexity of the material. Though the band structure of the studied quaternary crystals is not available in the literature, there are some evidence of splitting of the conduction and valence bands in the ternary crystals $Bi_{2-x}Sb_xSe_3$.[16] The occurrence of light and heavy electrons and holes, respectively, can account for the different behavior of transport parameters. Based on the presented experimental results it is difficult to ascertain which of the above explanations is more plausible.

For completeness, in Fig. 10, we show a comparison of the Hall mobility of electrons (samples 1) and holes (sample 5). The Hall mobility of electrons is considerably higher than that of holes throughout the temperature range investigated even though the respective temperature dependences are similar.

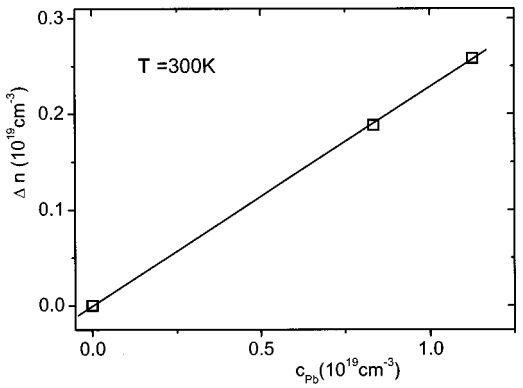

FIG. 8. Change in the concentration of electrons as a function Pb concentration c_{pb} at 300 K [$\Delta_n=n_0-n$, where n_0 and n are the concentration of the electrons in $(Bi_{0.75}Sb_{0.25})_2Se_3$ and Pb-doped samples, respectively].

E. *Figure of merit*

As already noted, Bi_2Te_3 and Sb_2Te_3 alloys are the materials of choice for room-temperature thermoelectric applications. The criterion by which one judges whether a material is useful as a thermoelectric is the so-called thermoelectric figure of merit $Z=\alpha^2/\rho\kappa$, where α is the Seebeck coefficient, ρ is the electrical resistivity, and κ is the thermal conductivity. Often, the dimensionless figure of merit ZT (T being the absolute temperature) is being used because, fortuitously, the values of unity represent the state-of-art room-temperature performance. In Fig. 11 we display the dimensionless figure of merit of all the samples studied. It is clear that the best material is still the basic ternary compound. Upon doping with Pb, the figure of merit slightly decreases. It should be noted, however, that in this work we did not aim at optimizing the thermoelectric performance, and much higher figures of merit might be achieved with appropriate doping. In particular, it would be interesting to explore the possibility of forming p-type materials based on Bi_2Se_3.

IV. CONCLUSION

Single crystals of quaternary $Bi_xSb_yPb_zSe_3$ compounds with the tetradymite structure were prepared by modified

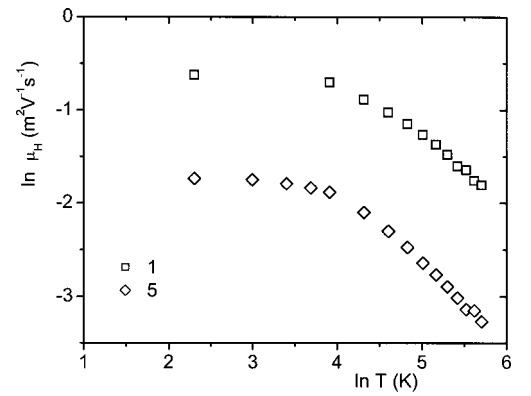

FIG. 10. Hall mobility as a function of temperature for samples 1 and 5.

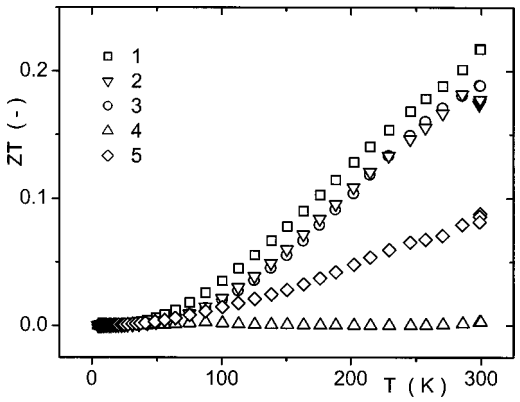

FIG. 11. Figure of merit as a function of temperature for crystals of $Bi_xSb_yPb_zSe_3$. The curves are numbered according to Table II.

Bridgman technique and were characterized by the detailed studies of the transport parameters such as electrical resistivity $\rho_{\perp c}$, Hall coefficient $R_H(B\|c)$, Seebeck coefficient $\alpha(\Delta T \perp c)$, and thermal conductivity $\kappa(\Delta T \perp c)$. The measurements indicate that by incorporating Pb in $Bi_{2-x}Sb_xSe_3$ one lowers the concentration of electrons and, at high levels of Pb, a crossover to *p*-type conduction takes place. This behavior can be understood in terms of point defects Pb'_{Bi} that produce holes.

ACKNOWLEDGMENTS

The authors gratefully acknowledge the support provided by the NSF Grant No. INT 020114, the ONR Grant No. N00014-03-1-0276, and the Ministry of Education, Youth and Sports of the Czech Republic under the Project No. MSM 0021627501.

[1] *CRC Handbook of Thermoelectrics*, edited by D. M. Rowe (CRC Press, Boka Raton, FL, 1995).
[2] A. Krost, in *Landolt–Bornstein, Group III Crystal and Solid State Physics*, New Series Vol. 17, edited by O. Madelung, M. Schulz, and H. Weiss (Springer, Berlin, 1983).
[3] M. Stordeur, K. K. Ketavong, A. Priemuth, H. Sobotta, and V. Riede, Phys. Status Solidi B **169**, 505 (1992).
[4] J. A. Woollam, H. Beale, and I. L. Spain, Phys. Lett. **41A**, 319 (1972).
[5] H. Koeller and A. Fabricius, Phys. Status Solidi B **71**, 487 (1975).
[6] P. Lošťák, Č. Drašar, H. Suessmann, P. Reinshaus, R. Novotný, and L. Beneš, J. Cryst. Growth **179**, 144 (1997).
[7] S. Karamazov, J. Horák, J. Navrátil, and P. Lošťák, Cryst. Res. Technol. **32**, 249 (1997).
[8] P. Lošťák, L. Beneš, S. Civiš, and H. Suessmann, J. Mater. Sci. **25**, 277 (1990).
[9] P. Lošťák, Č. Drašar, A. Krejčová, L. Beneš, J. S. Dyck, W. Chen, and C. Uher, J. Cryst. Growth **222**, 565 (2001).
[10] V. G. Kuznetsov, K. K. Palkina, and A. A. Reshchikova, Izv. Akad. Nauk SSSR, Neorg. Mater. **4**, 670 (1968).
[11] G. Offergeld and J. van Cakenberghe, J. Phys. Chem. Solids **11**, 310 (1959).
[12] J. Horák, J. Navrátil, and Z. Starý, J. Phys. Chem. Solids **53**, 1067 (1992).
[13] T. Plecháček, J. Navrátil, and J. Horák, J. Solid State Chem. **165**, 35 (2002).
[14] N. Frangis, S. Kuypers, C. Manolikas, G. van Tendeloo, J. van Landuyt, and S. Amelinckx, J. Solid State Chem. **84**, 314 (1990).
[15] P. Lošťák, R. Novotný, J. Navrátil, and J. Horák, Cryst. Res. Technol. **28**, 1093 (1993).
[16] V. A. Kulbachinskii, N. Miura, H. Nakagawa, H. Arimoto, T. Ikaida, P. Lošťák, and Č. Drašar, Phys. Rev. B **59**, 15733 (1999).